Proceedings of ASME Turbo Expo 2011
GT2011
June 6-10, 2011, Vancouver, British Columbia, Canada

GT2011-45457

EFFECT OF TURBINE TIP LEAKAGE FLOWS ON EXHAUST DIFFUSER PERFORMANCE

Mohan Babu, Dinesh Bhatia, Ram Krishan Shukla,
A M Pradeep, and Bhaskar Roy
Department of Aerospace Engineering
Indian Institute of Technology, Bombay
Mumbai, India 400 076
Email: ampradeep@aero.iitb.ac.in

ABSTRACT
This paper describes numerical simulation of the effect of turbine exhaust flows on typical exhaust diffuser geometries. The study has been carried out on three different diffuser geometries. These diffusers have varying degrees of diffusion in the annular section. The studies were carried out at a Reynolds number of 7.7 x 10^5 based on the diffuser inlet hydraulic diameter. The performance of the diffusers was assessed in terms of total pressure loss and static pressure coefficient across the diffuser. The turbine exhaust flow was simulated by combining an injection scheme from the casing in to the main flow that changes the uniform diffuser inlet velocity profile to that of a typical turbine exhaust flow profile. It was observed that the presence of a realistic exhaust flow influences the diffuser performance compared to an axial inlet flow. The effect of the real flow seems to be to make it more resistant to adverse pressure gradients. The exit flow of the diffusers, studied earlier, with uniform axial inlet flow, showed massively separated regions at the diffuser delivery. The diffuser performances improved significantly with realistic simulation of turbine exhaust flow. The present study also reinforces the fact that the diffuser performance is highly sensitive to the quality of the inlet flow.

NOMENCLATURE
A	Diffuser cross-sectional area
AD1	Annular diffuser 1
AD2	Annular diffuser2
C_P	Static pressure recovery coefficient, $\frac{(p-p_{ref})}{q_{av1}}$
C_{Pi}	Ideal static pressure recovery coefficient, $1-\frac{1}{A_S/A_1}$
d	Inlet casing diameter of the annular diffuser
h	Height of the annulus at a given section
L	Total length of the diffuser
p	Static pressure
p_0	Total pressure
q	Dynamic pressure
r	Radial distance
Re	Reynolds number
ω	Total pressure loss coefficient, $\frac{(p_{01}-p_{0S})}{q_{av1}}$
x	Axial distance along the length of the diffuser

Subscripts
1	Annular diffuser inlet plane
av	Average
ref	Reference place
s	Any axial plane

INTRODUCTION
Turbine exhaust diffusers usually have a set of radial struts meant primarily for supporting the rotor shaft. The turbine exhaust flow interacts with these struts, leading to total pressure loss.

A diffuser is used to recover a large part of the kinetic energy present in an exhaust of a gas turbine. The outlet pressure of the diffuser is often fixed by utilization conditions in the land based turbines. This allows a lower static pressure at the turbine exit, which thereby increases the available power of the turbine and thermal efficiency of the cycle. Therefore, the diffuser is a critical component in a combined cycle power plant. It is in this context that efficient design of gas turbine exhaust diffusers gain significance.

Kline [1] developed the design methodology for straight walled diffusers. Later on Sovran and Klomp [2] developed performance charts for a variety of annular diffusers. These performance charts form the basic starting point for design of annular diffusers. Steven and Williams [3] studied the performance of annular diffusers subjected to different inlet conditions. Sultanian et al. [4] investigated the performance of an exhaust diffuser under full load and part load conditions. Their studies indicated that the inlet swirl initiates flow separation under part load conditions. The computational data was validated through experiments.

Ubertini and Desideri [5, 6] investigated the flow physics and the effect of struts on the performance of an annular diffuser. They observed that the presence of the struts increases the total pressure losses. Flelge et al [7] in their studies on the effect of swirl and tip leakage flows on the performance of conical diffusers, observed that high inflow swirl interacts with the struts and degrades the performance of exhaust diffusers. It was also reported that tip strong flow increased the static pressure recovery in the diffuser without struts. However, they observed a slight decrease in the pressure recovery with struts because of the adverse effect of the interaction of the profiled struts with the turbine tip leakage flow. Klub et al. [8] studied the influence of tip leakage flow by increasing the turbine tip gap in the simulations and observed that increase in tip gap increased diffuser performance by reducing casing separation, but however the turbine work output was observed to reduce because of the tip clearance losses. In their studies, the impact of tip leakage flows was assessed by considering two approaches, namely, the mixing plane approach and the frozen rotor approach. Michael et al. [9] observed the effect of tip leakage flow by blowing air into the diffuser and reported an optimum mass flow to be injected to be 4% of the main mass flow.

In a series of publications, Vassiliev et al [10-12] and Ishizaka et al. [13] carried out extensive computational studies using a commercial CFD package, on different diffuser geometries including some of those discussed in Sovran and Klomp [2]. Several turbulence models were tested in these computations. It was observed that the realizable κ-ε (with two zone near wall treatment) gave the best results when compared with the experimental data. Feldcamp and Birk [14] also reported the effect of inflow swirl on diffuser performance. They evaluated the performance using different turbulence models in their CFD studies. Sieker and Seume [15] reported the effect of inflow conditions like swirl, rotating wakes (from the turbine exit) and secondary flows on the diffuser performance. Pradeep et al. [16] carried out design modifications on the casing geometry of the annular + conical exhaust diffuser. It was reported that the diffuser performance is highly sensitive to inflow conditions (like swirl) as well as the casing divergence angle.

In this paper results of studies of simulated typical turbine exhaust flow at low speed have been described in some detail. The results are presented for three different forward diffuser geometries, with the aft conical geometry held constant. All of them have different degrees of divergence in the annular (forward) part of the diffuser. The tip strong turbine exhaust flow is simulated by using an injection scheme from the casing such that it introduces a swirling boundary layer in the main flow, which is axial. It is intended to be observed whether a tip strong turbine exhaust flow has any significant effect on the subsequent diffuser performance in terms of static pressure recovery, total pressure losses and greater flow uniformity.

GEOMETRY, GRID AND BOUNDARY CONDITIONS:

The grid generation and simulations were carried out using the commercial package ANSYS CFX©. The baseline diffuser geometry is shown in Fig. 1. The diffuser comprises of a two-part annular diffuser followed by a conical diffuser. The annular diffuser also has five radial struts (Fig 1). Out of these five struts, four struts have a symmetrical airfoil cross-section where as the fifth strut that is a utility strut (meant for carrying lubrication pipes etc) has a thicker trailing edge cross-section. Details of the struts and the annular diffuser geometry are given in Pradeep et al. [16]. The struts also have a backward lean. These have been indicated in Fig. 1. The conical diffuser is connected to a rectangular plenum as shown in the figure.

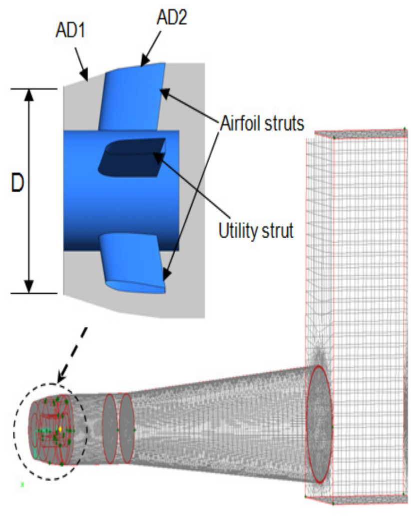

Fig. 1 Geometry and grid details: diffuser-0

In the two-part of the annular diffuser, tetrahedron grids were used as there are radial struts as well, whereas in the conical diffuser and the plenum, hexahedron grids were used. The total number of grids was about 3 million and the average y^+ in the diffuser section was around 4. The convergence criterion was fixed at 10^{-5} for the residuals. SST κ-ω turbulence model was used in the present study. This was based on Klub et al. [8] as well as using experience from CFD runs with other turbulence models. At the inlet to the domain, total pressure and velocity components are specified. For the injector flow, total pressure was specified at the inlet of the injector to achieve the desired injection mass flow rates.

EXPERIMENTAL SET-UP:

The experiments were performed in a low speed rig (Fig. 2). An axial fan at runs at 2400 rpm and delivers a air mass flow of 8 kg/s. The fan delivery flow is straightened using a set de-swirler vanes and a mesh to crate uniform axial flow delivery. The Reynolds number based on the diffuser inlet hydraulic diameter is 7.7 x 10^5. Measurements were taken at 6 locations indicated by planes 0-0 to 5-5. Wall static pressure taps were provided along the diffuser walls from inlet (plane1) to exit (plane 5). The total pressure was measured using kiel probes of 6 mm diameter. These kiel probes were designed to be insensitive to flow angles up to ±50 degrees. The kiel probes have an accuracy of 1 %. For boundary layer measurement, a boundary layer pitot probe of 0.5 mm with a flattened tip was used. The flow angles were measured using a nulling type 3-hole probe. Digital micromanometers and scanivalves (Scanivalve Corp, US) were used. The measured accuracies of these instruments were 1 % of full scale. For probe traverse, a precision traverse with a pitch of 0.5 mm was used.

RIG SIMULATION: The turbine exhaust flows carry tip strong swirling flow embedded within the velocity profile. This modified velocity profile carries an energized swirling boundary layer. This has been simulated by using a suitably designed injector. In the present rig study,

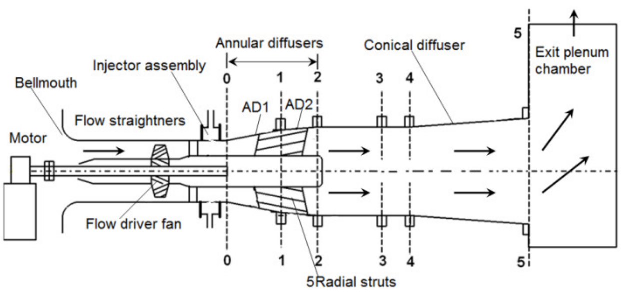

Fig. 2 Schematic of the test rig

In the present rig study, an annular injector was placed after the de-swirler, ahead of the annular diffuser (i.e. before 0-0). A schematic of the test rig is shown in Fig.2. This injector (Fig.3) alters the inlet velocity profile such that the uniform axial velocity field is modified to a velocity profile similar to that of a typical turbine exhaust flow. The injector gives a swirl in a direction opposite to that of the rotor rotation reminiscent of a typical turbine exhaust flow. A schematic of the injector is shown (Fig. 3).

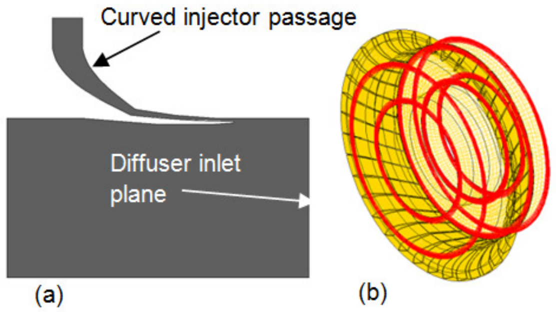

Fig. 3 Details of (a) Injector geometry and (b) meshing of the injector section

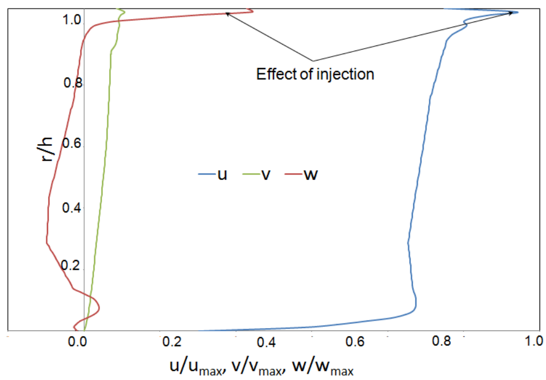

Fig. 4 Velocity profiles at the diffuser inlet

The diffuser inlet velocity profile generated by the injector is shown in Fig. 4 showing the modified velocities field with tip strong flow near the casing.

RESULTS AND DISCUSSION

The experiments were initially carried out on a baseline two-part exhaust diffuser (Diffuser-0). The geometric details are described elaborately in Pradeep et al [16]. Validation of the CFD results using experimental data was also performed on this diffuser. The performance of the diffuser was assessed based on the (i) static pressure recovery, (ii) the total pressure loss and (iii) the velocity uniformity along the length of the diffuser. As reported in Pradeep et al. [16], the annular diffuser is designed to rapidly diffuse the flow and hence the static pressure coefficient must increase steeply. Figure 5 shows the static pressure distribution along the length of the diffuser with the annular injection. The static pressure varies in a similar manner as discussed above. However, the static pressure all along the diffuser length is significantly higher than that (for diffuser-0) without injection. Clearly, the enhanced static pressure rise is one of the benefits of injection. Figure 5 also shows the static pressure distribution data from the experiments. The experimental data validates the CFD predictions, as evident from the good agreement between the two sets of data.

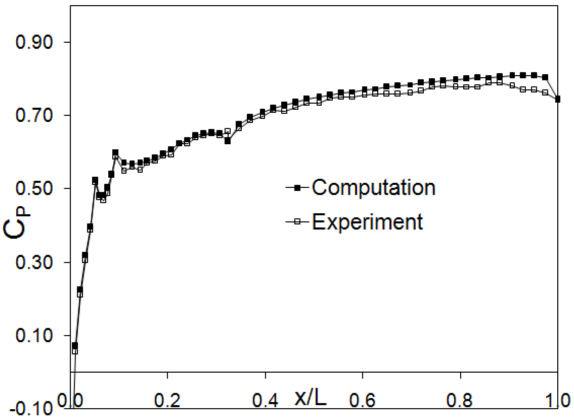

Fig. 5 C_P distribution along the diffuser

Figure 5 also shows the experimental data points for an injected inlet swirl, similar to that used in the CFD simulations. The CFD simulations match well with the experimental data in the initial part of the diffuser up to about x/L=0.45. The trends of the CFD simulations after wards slightly over predicts compared to the experimental data.

Figure 6 shows the radial total pressure loss coefficient distribution at station 2-2 (refer Fig. 2), using experimental data as well as from computations. The data shown is at one of the circumferential locations. Both sets of data agree well in terms of trend of the loss distribution. Near the casing and the hub, high values of loss can be observed. This is due to the viscous losses occurring in the boundary layer, with higher loss near the casing due to additional effect of adverse pressure gradients (casing diffusion). It can also be observed that the experimental data and computational data agree better in the region away from the walls.

The total pressure loss coefficients were also measured and computed at other axial locations downstream. In the conical diffuser section, the agreement between the experimental data and computations were not as good as is seen at stn.2-2 (Fig. 6). This disagreement was because, in the conical diffuser, regions of separated flow exist. Since experimental measurements were time averaged and were at discrete radial locations, data at these locations were not in good agreement with CFD simulation.

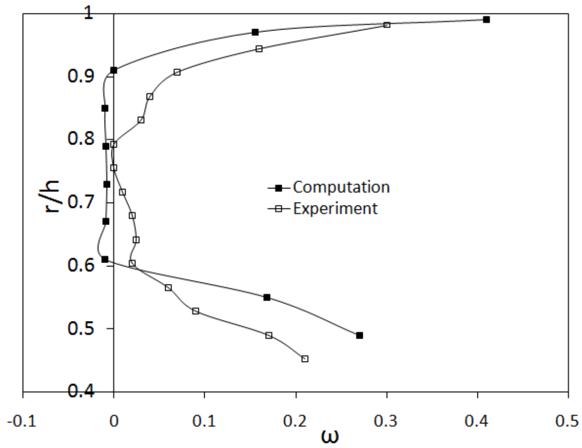

Fig. 6 Total pressure loss distribution at 2-2

Figure 7 shows a CFD comparison of near-casing velocity vectors for the annular diffuser, without and with inlet flow modification. As can be clearly seen, with uniform flow a low momentum region develops on one of the sides of the airfoil struts. However with tip-strong inlet flow no such low momentum region is observed. The energised boundary layer (tip strong flow) prevents flow separation even though the flow impinges the struts at an angle of attack.

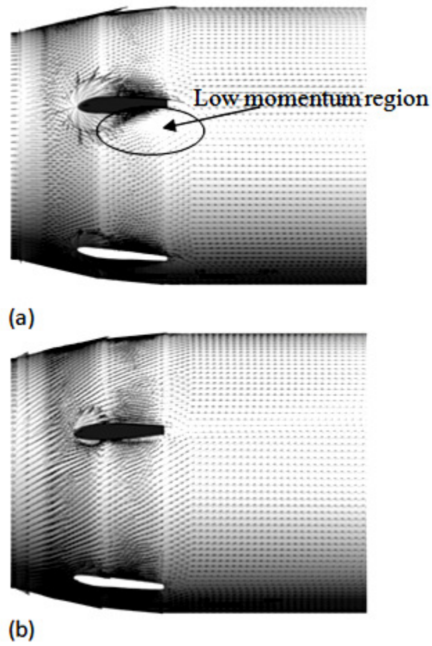

Fig. 7 Near-field vectors (a) with uniform inlet flow (b) with tip-strong inlet flow

Contours of velocity vectors along the length of the diffuser are shown in Fig. 8 for the diffuser with tip-strong flow. The wake of the utility strut is prominently visible. However this wake dissipates rapidly and does not initiate a massive separated region as was observed for the diffuser without

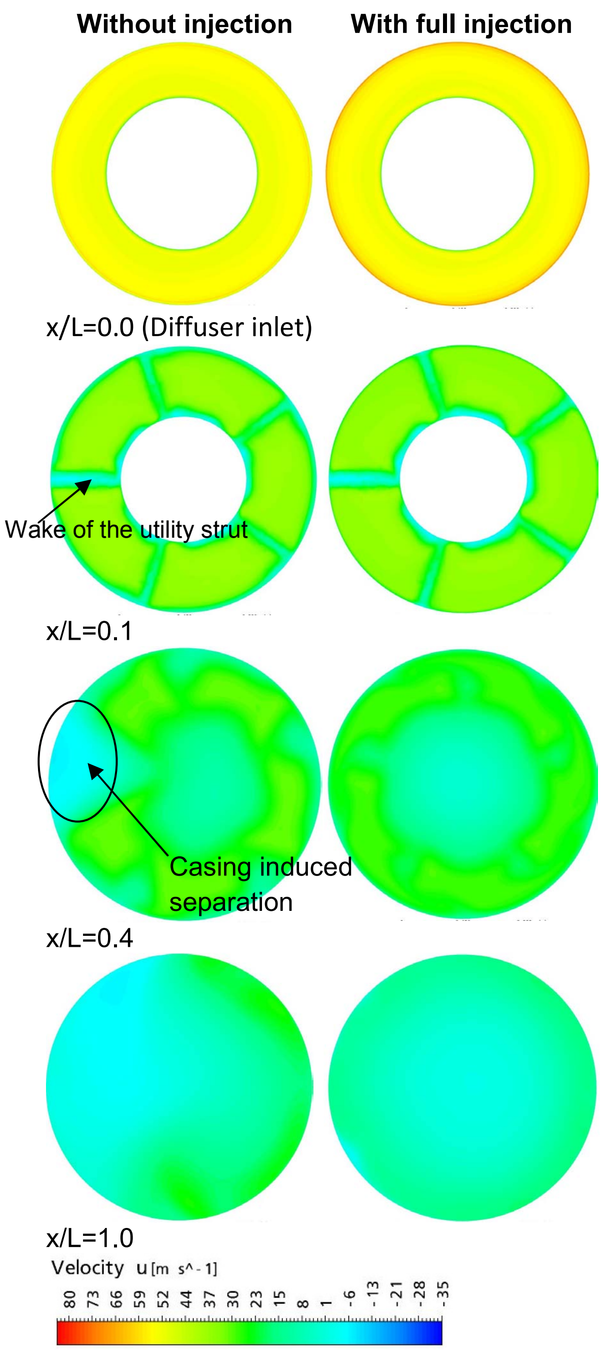

Fig. 8 Velocity contours of diffuser-0

injection (Pradeep et al. [16]). The base flow originating from the hub of the diffuser persists all the way up to the end of conical diffuser, growing in size along the diffuser length. However with tip-strong inlet flow, the flow at the conical diffuser exit is quite uniform with a low velocity core flow. Pradeep et al. [16] had reported, that for uniform axial inlet flow, a massively separated region at the conical diffuser exit with a major portion of the diffuser exit flow occupied by separated, re-circulating flow. This means a substantial total pressure loss. From CFD analysis it is expected that with introduction of tip-strong flow there would be an improvement in the static pressure rise and reduction in the total pressure loss. This would be discussed in detail in the subsequent sections.

The effect of tip-strong flow on the performance of the diffuser was further investigated using varying amounts of simulated injection. Full injection and partial injection were used to recreate varying strength of tip-strong flow. Figure 9 shows the velocity distributions at x/L of 0.3 for part and full injection. It can be seen that reducing the strength of tip-strong flow does not deteriorate the diffuser performance significantly. However, at nominal injection, the performance of the diffuser is seen to be substantially affected. This is seen in Fig. 10 that shows the velocity contours at the conical diffuser exit. Both the injection rates showed improved diffuser performance, but not as significantly as for the full injection case.

Fig. 9 Velocity field at x/L=0.3 (diffuser-0)

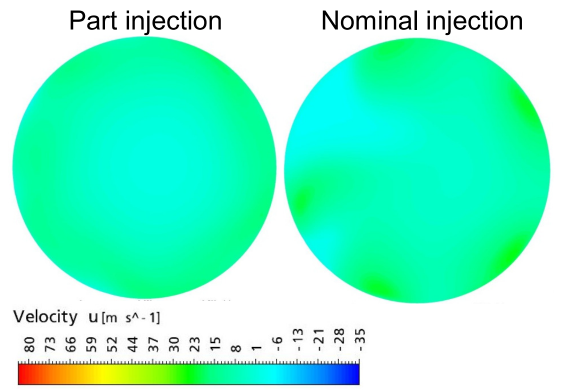

Fig. 10 Velocity field at x/L=1.0 (diffuser-0)

The overall simulation effect of varying strength of tip-strong flow in terms of static pressure coefficient, C_P and total pressure loss coefficient, ω, as obtained from CFD analysis, can be seen in Fig. 11. The C_P and K values shown in the figure are area averaged at various circumferential planes in axial direction. C_P rises steeply from x/L=0 to x/L=0.02, which correspond to the front of the annular diffuser. The C_P curve droops thereafter slightly due to the presence of struts. The pressure recovery values of the without and with tip-strong flow in the annular diffuser remain almost the same. This is because the flow does not actually separate in this annular diffuser section. The difference between the diffuser performance without and with tip-strong flow is clearly seen in the conical diffuser section. Figure 10 shows the velocity distribution at the conical diffuser exit for part and nominal injection. All the cases with injection lead to improved diffuser performance. In the cases with full and part injection, no flow separation was observed at the conical diffuser exit. With nominal injection, however, there are small pockets of separated flow as seen in Fig. 10. This also led to decrease in the static pressure recovery. Figure 11 compares all the simulation results with ideal C_P for diffuser-0. Diffuser with full injection had a C_P distribution closest to the ideal C_P.

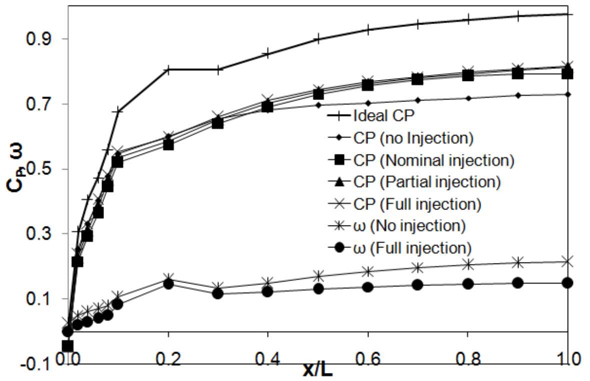

Fig. 11 Static pressure and total pressure loss distributions

Other diffuser geometries:

The effect of turbine tip leakage flows on diffuser-0 was discussed in the preceding sections. It will be interesting to see the effect of tip-strong flows on some other diffuser geometries. CFD studies on two such geometries will be discussed in the following sections.

Diffuser-1:

Pradeep et al. [16] had discussed some diffuser geometries that had substantially improved performance than the diffuser-0. Borne out of those CFD studies two annular (forward) diffuser geometries have been created.

One of them is a three-part annular diffuser, which begins with shallow diffusion, followed by a sharp diffusion and ends with shallow diffusion. This may be called Diffuser-1. This diffuser geometry is subjected to simulated flows – firstly, the uniform axial flow and, later with simulated tip-strong flow.

Figure 13 shows the velocity vectors near the casing of the forward diffuser with and without tip-strong flow. With uniform axial inlet flow there is a small pocket of low momentum flow near the trailing edge of the normal strut. The magnitude of this is lower than what was observed in diffuser-0. With tip-strong flow, this low momentum region disappears. Contours of velocity along the axis of the diffuser without and with injection are shown in Fig. 14. A small region of flow separation persists at the conical diffuser exit. With injection, there was no flow separation observed and the exit flow uniformity appears similar to that observed in diffuser-0 with injection.

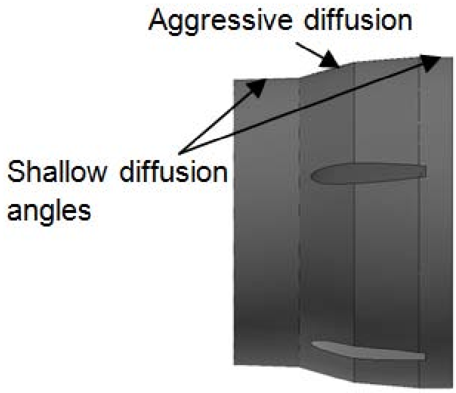

Fig. 12 Three part annular diffuser-1

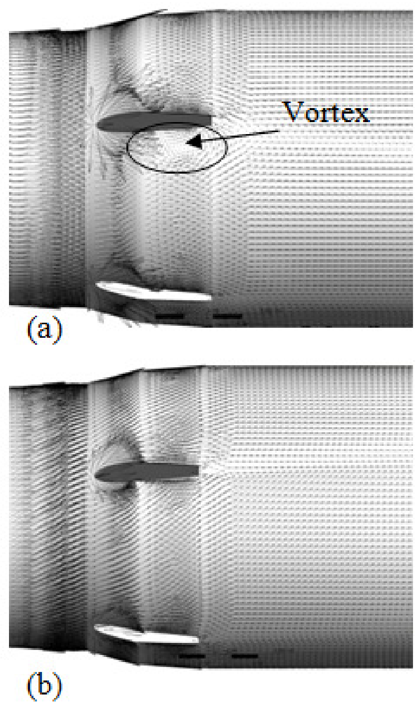

Fig. 13 Near-casing velocity vectors (a) without and (b) with injection (diffuser-1)

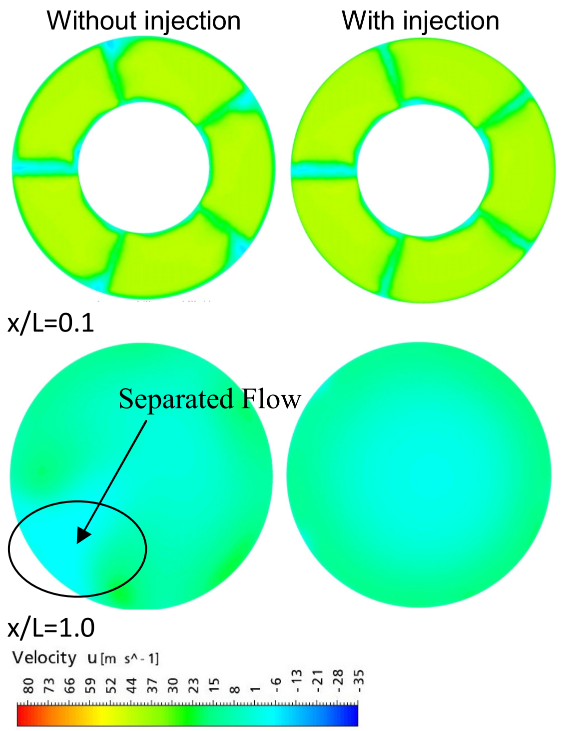

Fig. 14 Velocity contours along the length of the diffuser-1

The improvement in flow quality in the diffuser-1 even without injection (as compared with diffuser-0, Fig.8) is also evident in Fig. 14.
The overall effect of injection in terms of C_P and K is shown in Fig. 15. It can be observed that there is only a marginal increase in C_P from x/L= 0 to x/L=0.02. This is because of the shallow initial diffusion angle. This is followed by a sudden drop in C_P from x/L=0.02 to x/L=0.04. Subsequently, a steady increase in the C_P till the end of the diffuser with different slopes corresponding to the changes in diffusion angle is observed. The sudden drop in C_P between x/L=0.02 to 0.04 can be explained by comparing it with the ideal C_P value. The ideal C_P takes only the area into account whereas flow acceleration caused by the shape of the struts was not taken into account, which actually causes the reduction in the C_P.
From Fig. 15, it is seen that the difference between the C_P for the diffuser-1 without and with injection is marginal. This is also reflected in the marginal difference seen in the total pressure loss variation. This is because, the flow was rather well behaved in the diffuser-1 even without injection, except for a small pocket of separated flow at the end of the conical diffuser.
Therefore the presence of a tip-strong flow created artificially by the injection scheme does not add significantly to the diffuser performance. In the diffuser-1 with injection (as seen from Fig. 13), the separated flows around the struts is eliminated, resulting in a marginally improved performance.

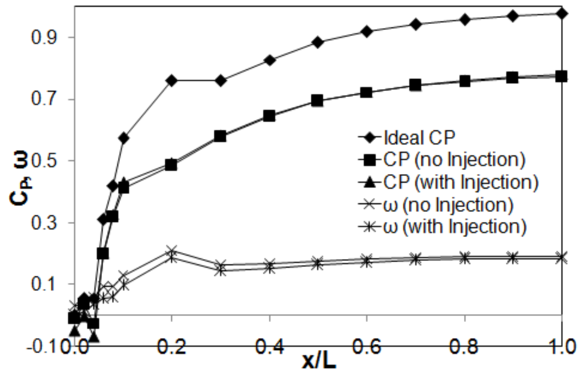

Fig. 15 C_P and ω distribution for diffuser-1

Diffuser-2:
It is known that the presence of the struts lead to substantial total pressure losses. The magnitude of these losses also depends upon the velocity of the inflow. Therefore, if the inflow is decelerated using an aggressive forward diffuser before the flow encounters the struts, total pressure losses due to the struts can be minimized. Based on this argument, a one-part diffuser geometry with a aggressive outer annulus divergence has been studied (Diffuser-2). Such a diffuser geometry, however, has an inherent high risk of flow separation. Figure 16 shows the geometry of this diffuser. The divergence angle employed in this case is higher than the divergence angles anywhere either in the diffuser-0 or in the diffuser-1.

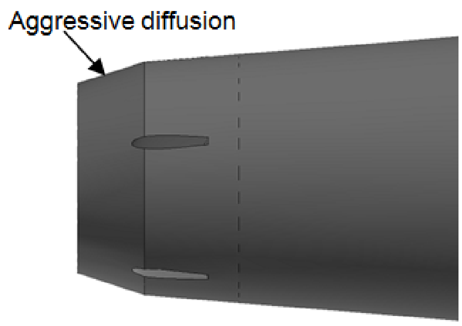

Fig. 16 One-part annular diffuser-2

Figure 17 shows the velocity vectors near the casing of diffuser-2 without and with separation. It is observed that without injection, flow separation initiates even before the flow encounters the struts. This was eliminated with injection (Fig. 17b). Interestingly, near the hub, flow separation was initiated in the case of diffuser-2 with injection. This can be seen from Fig. 18. From Fig. 18a, it is clear that without uniform inflow, the flow near the strut hub did not experience any separation. With tip-strong flow, however, flow reversal near the leading edge of the airfoil struts was observed. Injection from the casing only energised the flow in that region, whereas the hub flow had insufficient momentum to withstand the adverse pressure gradients. This can also be seen in the subsequent paragraph which describes the velocity distribution along the length of the diffuser.

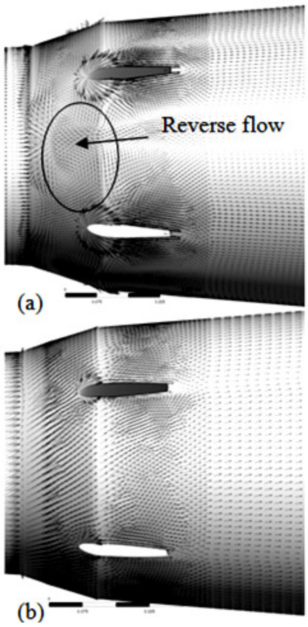

Fig. 17 Near-casing velocity vectors for diffuser-2

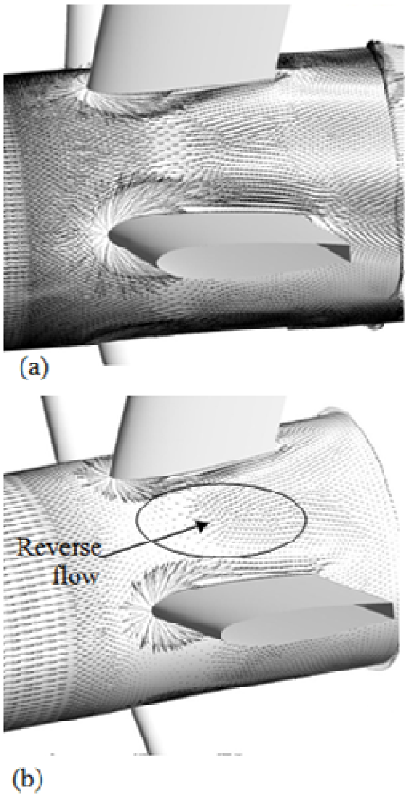

Fig. 18 Near-hub velocity vectors for diffuser-2

Contours of velocity at various axial planes along the length of the diffuser are shown in Fig. 19. At x/L=0.1, which corresponds to the plane at the exit of the struts, what was discussed in regard to Fig. 17 and 18 can be visualized. For the diffuser without injection, separated regions of flow can be observed near the casing. With injection, separation is observed near the hub, while the casing flow is well behaved. In the conical diffuser section, diffuser-2 without injection has a highly non-uniform velocity distribution due to a large part of the flow under the influence of separation. With injection, there is a significant improvement in the flow uniformity even at the conical diffuser exit.

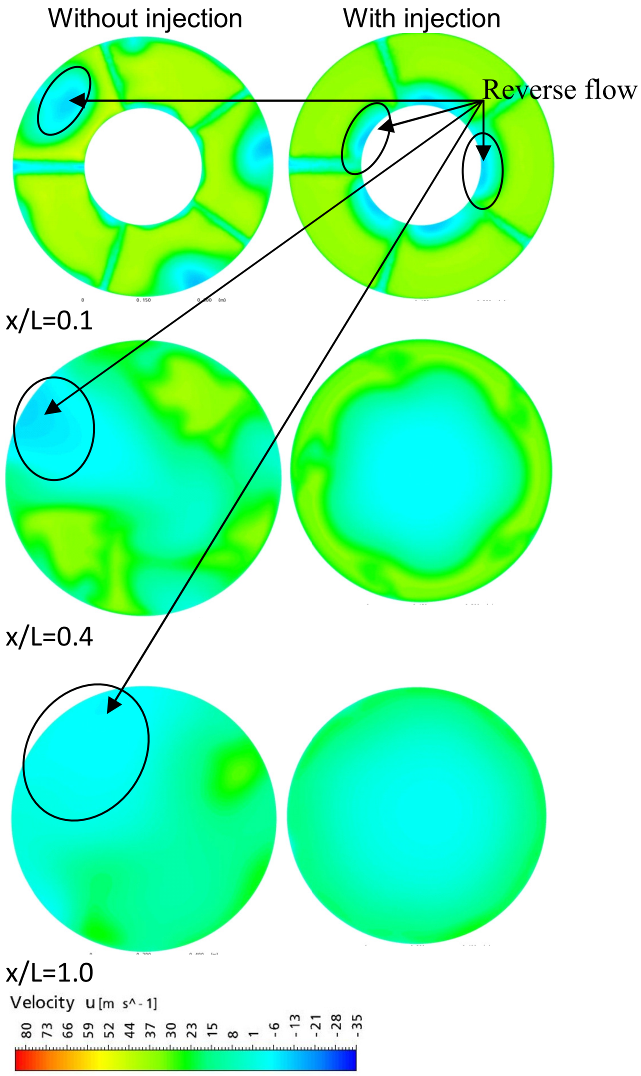

Fig. 19 Velocity contours along the length of diffuser-2

Figure 20 gives the overall effect of injection on the performance of diffuser-2. The ideal C_P is also shown in the figure. The performance of the diffuser has improved all along the length of the diffuser in terms of improved static pressure recovery and lower total pressure loss. This is in contrast with diffuser-1, where there was hardly any noticeable effect of injection. In diffuser-2, flow separation was initiated within the annular diffuser itself and hence use of injection improved the flow quality in both the annular diffuser section as well as in the conical diffuser. In diffuser-1, the flow was well behaved even in absence of any injection and energizing the boundary layer had negligible impact on the diffuser performance.

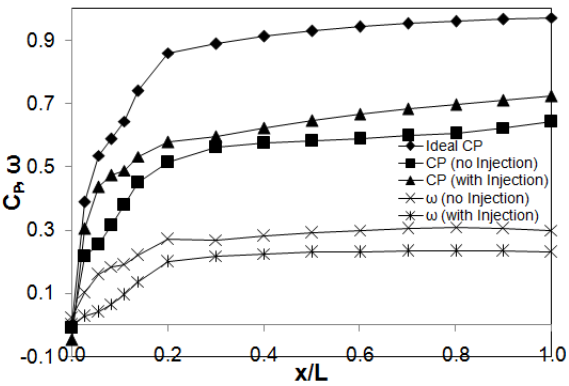

Fig. 20 Cp and ω distribution of diffuser-2

Table 1 summarizes the performance of the three diffusers without and with simulated tip-strong flow. The performance parameters listed are C_P and ω at the conical diffuser exit. With introduction of tip-strong flow, in the case of diffuser-0, about 12% increase in C_P and 30% reduction in ω was observed. Diffuser-1 has a basically better performance than diffuser-0. With injection, the performance improvement in diffuser-1 was marginal. Diffuser-2 had a poor overall performance compared to the two other diffusers. With injection C_P, however, improved by about 12% and ω reduced by 22% at stn 5-5, compared to the flow without injection.

Table 1. Summary of results of the three diffuser geometries - at stn 5-5

Inflow condition	Performance parameters	2-part Diffuser	3-part Diffuser % change	1-part Diffuser % change
No injection	Cp	Cp Base	+5.7%	-11.8%
	ω	ω Base	-10.3%	+40%
With injection	Cp	+12%	+7.3%	-0.5%
	ω	-30%	-14%	+8%

CONCLUSIONS

In the present study, a detailed CFD analysis of the flow characteristics of three turbine exhaust diffuser geometries, in absence and in presence of turbine exhaust tip-strong flows, was carried out. Turbine tip strong flow was simulated using an annular injection (with a skew) scheme, applied from the casing. For the first diffuser configuration (diffuser-0), experimental validations of the computational studies have been carried out. The CFD predictions were satisfactorily validated using the experimental data. Two other diffuser geometry configurations involving re-design of the annular part of the diffuser were also analysed without and with tip-strong flows. All the diffusers had varying degrees of divergence in the annular part of the diffuser.

Based on the present CFD study, the following conclusions can be drawn:

1. Diffuser performance is highly sensitive to inflow conditions. Typical turbine exhaust flows carry a thin tip-induced casing boundary layer (tip-strong flow), which energizes and enables the casing flow to overcome adverse pressure gradients.
2. It can be seen from the Figs 5, 11 and 15 that C_p development of three diffusers proceeds quite differently. When tip-strong flow is applied, the starting diffuser-0 at the end of the 2-part annular diffuser by station 2-2 achieves a C_p of 0.5, whereas the 3-part diffuser achieves C_p of only 0.42 and the 1-part diffuser achieved a C_p of 0.53.
3. In diffuser-0, annular casing injection lead to substantial performance improvements: 12% in static pressure recovery C_p and 30% reduction in total pressure loss, ω as estimated by CFD simulation at stn 5-5.
4. The 3-part annular diffuser (Diffuser-1) performance even with uniform axial inlet flow was better behaved than that of diffuser-0. Introduction of tip-strong flow caused only a marginal improvement in its overall performance (2.3 % in C_p and 3.5% in ω at station 5-5). Thus, studies on 3-part diffuser-1 revealed that amongst all the diffusers geometries that were studied this one promotes relatively well controlled diffusion with uniform inflows, the introduction of tip strong flow does not improve the performance significantly. Thus the 3-part diffuser-1 benefits minimum from a tip-strong inlet flow.
5. The 1-part diffuser-2, which is intended to promote fast diffusion in the forward strutted diffuser, indeed actually benefits maximum initially from introduction of a tip-strong inlet flow [ref-2 above]. However, attempted aggressive diffusion in the strutted annulus creates nascent separation tendencies which later in the conical diffuser grow in to large separation zones, causing lower C_p and higher ω at the diffuser exit plane 5-5.
6. Benefits of casing injection induced tip-strong flow are evident only when the diffuser flow shows signs of separation tendencies initially in the annular strutted forward diffuser (due to high diffusion angles). This was evident from the substantial improvements observed in the case of diffuser-2 by station 2-2.

7. Thus, when the diffuser inlet flow is expected to be uniform (at the turbine operating points) one may use a 3-part diffuser like diffuser-1. On the other hand, if the diffuser inlet contains a highly tip-strong flow one may consider using diffuser-2, at it may provide reasonable diffusion at a shorter length.

ACKNOWLEDGMENTS

The authors would like to thank Siemens Energy Inc., Orlando, USA, for funding this work and for their permission to publish this paper. The stimulating discussions and various suggestions from Mathew Montgomery, Tito Islam and Bruce Smith, all of Siemens Energy Inc., USA are gratefully acknowledged.

REFERENCES

[1] Kline. S. J., Abbott. D. E. and Fox. R. W., “Optimum design of straight-walled diffusers,” ASME Journal of Basic Engineering, Vol. 91, 1959, pp. 321-330.

[2] Sovran, G. and Klomp, E.D., 1967, “Experimentally Determined Optimum Geometries for Rectilinear Diffusers with Rectangular,” Conical or Annular Cross-Section, Fluid Mech. of Int. Flow, Symp., pp.270-319.

[3] Stevens, S.J. and Williams, G.J. 1980, “The Influence of Inlet Conditions on the Performance of Annular Diffusers,” Journal of Fluids Engineering, Transactions of the ASME, Vol.102, pp.357-363.

[4] Sultanian, B. K., Nagao, S. And Sakamoto, T., 1999, "Experimental and Three-Dimensional CFD Investigation in a Gas Turbine Exhaust System," Journal of Engineering for Gas Turbines and Power, 121(2) pp.364-374.

[5] Ubertini, S. and Desideri, U., 2000, “Experimental Performance Analysis of an Annular Diffuser with and without Struts,” Experimental Thermal and Fluid Science, Vol.22, pp.183-195.

[6] Ubertini, S. and Desideri, U., 2000, “Flow Development and Turbulence Length Scales within an Annular Gas Turbine Exhaust Diffuser,” Experimental Thermal and Fluid Science, Vol.22, pp.55-70.

[7] H.-U. Flelge, W. Riess and J. Seume, 2002, “Swirl and Tip Leakage Flow Interaction with Struts in Axial Diffusers,” Proceedings of ASME Turbo Expo, Amsterdam, Netherlands, GT2002-30491.

[8] Klub, D., Wiedermann, A. and Stoff, H., 2008, “Effect of Wakes and Secondary Flow on Re-Attachment of turbine Exit Annular Diffuser Flow,” Proceedings of ASME Turbo Expo, Berlin Germany, GT2008-50211.

[9] Michael H., Tajc, L., Krejcik, J., Bednar, L., Sedlak, K. and Linhart, J., “Exhaust hood for steam turbine - single-flow arrangement,” Front Energy Power Engg China, 2009, pp 1-9.

[10] Vassiliev, V., Irmisch, S. and Florjancic, S., 2002, “CFD Analysis of Industrial Gas Turbine Exhaust Diffusers,” ASME, IGTI, Turbo Expo, Amsterdam, Netherland, GT2002-30597.

[11] Vassiliev, V.I., Volkov, D.V., Zaitsev, S.A. and Lyubimov, D.A., 1997, "Numerical Simulation of Channel Flows by One-Equation Turbulence Model", Journal of Fluids Engineering, Vol.119, pp.885-892.

[12] Vassiliev, V., Irmisch, S, Claridge, M. and Richardson, D.P., 2003, “Experimental and Numerical Investigation of the Impact of Swirl on the Performance of Industrial Gas Turbine Exhaust Diffusers,” Proceedings of ASME Turbo expo, Atlanta Georgia USA, GT2003-38424.

[13] Ishizaka, K., Wakazono, S., Yuri, M. and Takahashi, R. “CFD studies of industrial gas turbine exhaust diffusers,” TS-026, Proceedings of International Gas Turbine Congress 2003, Tokyo, Nov 2-7, pp. 1-8, IGTC 2003.

[14] Feldcamp, G.K. and Birk, A.M., 2008, “A Study of Modest CFD Models for the Design of an Annular Diffuser with Struts for Swirling Flow,” Proceedings of ASME Turbo Expo, Berlin Germany, GT2008-50605.

[15] Sieker, O. and Seume, J.R., 2008, “Influence of Rotating Wakes on Separation in Turbine Exhaust Diffusers,” Journal of Thermal Science, Vol.17, No.1, pp.42-49.

[16] Pradeep, A.M., Roy, B., Vaibhav, V. and Srinuvasu, D., 2010, “Study of Gas Turbine Exhaust Diffuser Performance and its Enhancement by Shape Modifications”, Proceedings of ASME TURBO EXPO, Glasgow, Scotland, GT2010-22088.

